Numerical Simulation of Thermal Stresses in Prismatic Concrete Beams Reinforced with FRP Bars under Low Temperatures

A. Zaidi[1], R. Masmoudi[2], S. Amara[1], M. Laidi[1] and S. Saci[1]

[1]Structures Rehabilitation and Materials Laboratory (SREML), University of Laghouat, Algeria
[2]Department of Civil Engineering, University of Sherbrooke, QC., Canada

Abstract. The thermal properties of fiber reinforced polymer (FRP) bars particularly in the transverse direction are higher than those of hardened concrete and steel bars. The difference in transverse thermal characteristics between FRP bar and concrete generates radial tensile stresses within concrete at the interface of FRP bars/concrete under low temperatures. These thermal stresses may cause circumferential cracks in concrete at the interface and eventually the reduction of the bond that can affect significantly the serviceability of reinforced concrete structures. This paper presents a nonlinear numerical simulation of thermal stresses in prismatic concrete beams reinforced with glass FRP (GFRP) bars submitted to low temperatures when the confining action of concrete is asymmetric. The non linear numerical analysis shows that the first circumferential cracks start to develop within concrete at FRP bar/concrete interface at a temperature decrease ΔT_{cr} varied between -30 ℃ and -25 ℃ for prismatic concrete beams reinforced with GFRP bars having a ratio of concrete cover thickness to FRP bar diameter (c/d_b) varied from 1.0 to 3.2. Furthermore, the depths of circumferential cracks propagated from the interface through the concrete cover increase with the decrease of the thermal load ΔT (from -25 ℃ to -50 ℃). These depths did not reach the outer surface of the concrete cover under low temperatures up to -50 ℃. Also, the radial tensile stress at FRP bar/concrete interface increases with the increase in the ratio c/d_b. The cracking thermal loads and thermal stresses predicted from nonlinear finite element model are compared to those evaluated with analytical models. Comparisons between numerical and analytical results in terms of cracking thermal loads and thermal stresses are presented.

1 Introduction

The use of fiber reinforced polymer (FRP) materials as a reinforcement in concrete structures has increased remarkably in recent years, because of their excellent resistance to corrosion, high tensile strength, low weight, electromagnetic neutrality, and high stiffness. Nevertheless, the thermal expansion of FRP bars in the transverse direction is higher than that of the hardened concrete. This difference in transverse thermal expansion between FRP bars and concrete may cause circumferential cracks within concrete at FRP bar/concrete interface under low temperatures. As a consequence, the serviceability of reinforced concrete structures can be reduced. Many experimental works were carried out on thermal effect on concrete structures reinforced with FRP bars [1-4]. However, numerical studies in this topic need more investigation particularly the effect of low temperatures on stress and strain distributions in concrete cover at the interface of FRP bar/concrete. This paper presents a nonlinear numerical simulation using ADINA software to investigate thermal stress distributions at the interface of concrete/FRP bars when the confining action of concrete surrounding FRP bar is asymmetric. This investigation has been carried out on prismatic concrete beams reinforced with glass FRP (GFRP) bars subjected to low temperatures (ΔT) up to -50 ℃. The nonlinear finite element analysis allows to determine the thermal loads (ΔT_{cr}) producing the first circumferential cracks within concrete at the interface of FRP bar/Concrete as a function of the ratio of concrete cover thickness to FRP bar diameter for reinforced prismatic concrete beams used. The thermal stresses and cracking thermal loads predicted from the numerical model are compared with those obtained from analytical models.

2 Non-linear finite element analysis

2.1 Finite element model

A nonlinear numerical simulation was carried out utilizing ADINA software to analyse thermal stress distributions in prismatic concrete beams reinforced with glass FRP (GFRP) bars submitted to a temperature decrease (ΔT) varied from 0 to -50 ℃ with an increment of -5 ℃. The ratio of concrete cover thickness to FRP bars (c/d_b) used is varied from 1 to 3.2, as shown in figure 1 and Table 1. The prismatic concrete beam was modeled by means of two dimensional plane stress elements because of the constant of axial deformations. The study was carried out only for the half of the cross section because of the symmetric of the cross-section of the prismatic concrete beam with respect to z-z axis, as shown in figure 1a and 1c. The meshing of the both

GFRP bar and concrete (Figure 2) was carried out using triangular elements with 6 nodes.

GFRP bars used in this study had a linear elastic behavior. The mechanical properties of GFRP bars determined experimentally [3] are presented in Table 2. The modulus of elasticity (E_t) and Poisson's ratio (ν_{tt}) of GFRP bars in the transverse direction evaluated theoretically using the rule of mixture were found to be equal to 7.1 GPa and 0.38, respectively. The transverse and the longitudinal coefficients of thermal expansion (CTE) of GFRP bars for the five FRP bar diameters tested were found to be equal to $\alpha_t = 33 \pm 4 \times 10^{-6}/°C$ and $\alpha_l = 8 \pm 1 \times 10^{-6}/°C$ in average, respectively. The concrete used in this study was considered to have a non-linear behavior. The mechanical properties of the concrete are reported in Table 3. The average tensile strength (f_{ct}) of concrete was determined by splitting tests and the average compressive strength (f'_c) was evaluated by standard compression tests. The modulus of elasticity of concrete (E_c) was determined according to CAN/CSA-S806-02 guidelines [5], while the Poisson's ratio of concrete (ν_c) was assumed 0.17. The coefficient of thermal expansion (CTE) of concrete was determined by experimental tests and was found to be equal to $11.6 \pm 2.1 \times 10^{-6}/°C$.

Fig. 2. Meshing of the both concrete and GFRP bar

Table 1. Detail of prismatic concrete beams reinforced with GFRP bars.

Specimens	Spec. width b_1 [mm]	Spec. Height h [mm]	Bar diameter d_b [mm]	Concrete cover thickness c [mm]	c/d_b
P.#10.20*	76	100	9.5	20	2.1
P.#10.25	76	100	9.5	25	2.6
P.#10.30	76	100	9.5	30	3.2
P.#13.20	76	100	12.7	20	1.6
P.#13.25	76	100	12.7	25	2.0
P.#13.30	76	100	12.7	30	2.5
P.#16.20	76	100	15.9	20	1.3
P.#16.25	76	100	15.9	25	1.6
P.#16.30	76	100	15.9	30	1.9
P.#19.20	100	125	19.1	20	1.0
P.#19.25	100	125	19.1	25	1.3
P.#19.30	100	125	19.1	30	1.6
P.#25.25	100	150	25.4	25	1.0
P.#25.30	100	150	25.4	30	1.2
P.#25.35	100	150	25.4	35	1.4

*P : Prismatic concrete beam ; #10 : Nominal diameter GFRP bar; 20 : Concrete cover thickness in mm

A-A

(a)

(c)

$a = d_b/2$
$b = d_b/2+c$

GFRP bar

Concrete

380 mm

(b)

Fig.1. Prismatic concrete beam reinforced with GFRP bar modeled

Table 2. Mechanical properties of the GFRP bars

Bar diameter d_b, mm	Ultimate tensile strength f_{fu}, MPa	Longitudinal modulus of elasticity E_l, GPa	Longitudinal Poisson's ratio ν_{lt}
9.5	627 ± 22	42 ± 1	0.28 ± 0.02
12.7	617 ± 16	42 ± 1	0.28 ± 0.02
15.9	535 ± 9	42 ± 1	0.28 ± 0.02
19.1	600 ± 15	40 ± 1	0.28 ± 0.02
25.4	N/a	N/a	0.28 ± 0.02

Table 3. Mechanical properties of concrete

| Compressive strength f'_{c28}, MPa	Tensile strength f_{ct28}, MPa	Modulus of elasticity E_c, GPa
40 ± 3	4.1 ± 0.1	28 ± 2

2.2 Numerical Results

Figures 3 shows typical curves of radial tensile thermal stresses within concrete at FRP bar/concrete interface for prismatic concrete beams reinforced with GFRP bars, under low temperatures, having a ratio of concrete cover thickness to FRP bar diameter (c/d_b) equal to 1.2 and 2.5. It can be seen that the tensile stress increases with the decrease in the temperature variation (ΔT_{cr}) until -25 ℃ and -30 ℃ corresponding to ratios of c/d_b equal to 2.5 and 1.2, respectively. From these thermal loads ΔT_{cr} the radial tensile stress decreases abruptly because of the appearance of the first circumferential cracks within concrete at the interface, as shown in figure 4. It is noted that the depths of circumferential cracks propagated from the interface through the concrete cover increase with the decrease of the thermal load ΔT (from -25 ℃ to -50 ℃). These depths did not reach the external surface of concrete cover for temperature variations up to -50 ℃ (Figure 5). Table 4 presents the thermal loads ΔT_{cr} producing the first circumferential cracks within concrete at FRP bar/concrete interface versus the ratio of c/d_b varied from 1 to 3.2 for prismatic concrete beams reinforced with GFRP bars having asymmetric concrete confining action. It is observed that the circumferential cracking concrete appeared in concrete cover at thermal loads of -25 ℃ for c/d_b varied from 3.2 to 1.9 and -30 ℃ for c/d_b varied from 1.9 to 1.
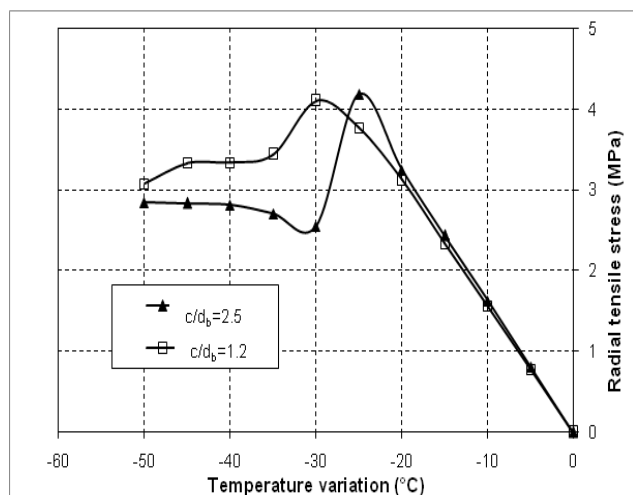
Fig. 3. Radial tensile stresses in concrete at concrete/FRP bar interface for prismatic concrete beams having c/d_b=1.2 and 2.5
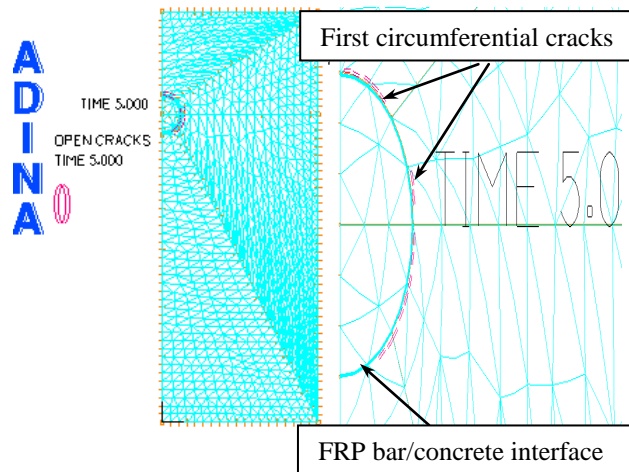
Fig. 4. Appearance of the first circumferential cracks within concrete at FRP bar/concrete interface at thermal load ΔT_{cr} (for concrete beams having c/d_b =2.5, ΔT_{cr} = -25 ℃)

(a) ΔT = -30 ℃   (b) ΔT = -50 ℃
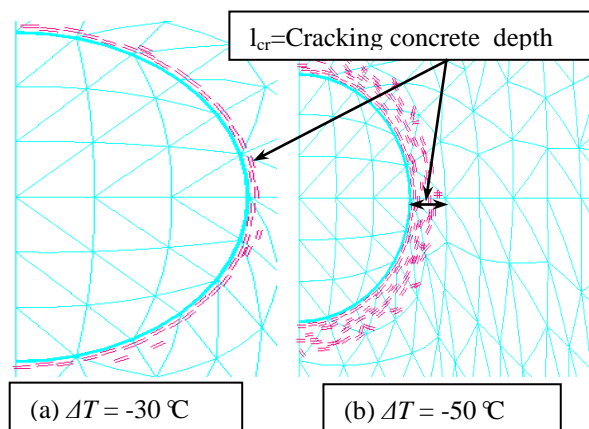
Fig. 5. Circular crown of circumferential cracked concrete formed at thermal loads -30 and -50 ℃ (for concrete beam having c/d_b =2.5)

Table 4. Non linear numerical thermal loads (ΔT_{cr}) producing the first circumferential cracks within concrete at FRP bar/concrete interface for prismatic concrete beams

c/d_b	ΔT_{cr} (℃)
$1.9 < c/d_b \leq 3.2$	- 25
$1 \leq c/d_b \leq 1.9$	- 30

3 Linear analytical analysis of thermal stresses

The thermal expansion of FRP bars in the transverse direction is higher than that of hardened concrete. This difference in transverse thermal expansion

generates radial pressure (P) at the interface of FRP bar/concrete under low temperatures (ΔT). This radial pressure creates tensile stresses within concrete. From the analytical models carried out by Rahman et al. (1995) [6] and Masmoudi et al. (2005) [3], the radial tensile stress (σ_ρ) in a concrete element situated at a radius ρ from the center of concrete cylinder reinforced with FRP bar due to radial pressure P, is given by:

$$\sigma_\rho = \frac{P}{r^2 - 1}\left(1 - \frac{b^2}{\rho^2}\right) \qquad (1)$$

Where $r = b/a$ is the ratio of concrete cylinder radius ($b = c + d_b/2$) to FRP bar radius ($a = d_b/2$), as shown in figure 1c; P is the radial pressure at FRP bar/concrete interface which is given by:

$$P = \frac{(\alpha_t - \alpha_c)\Delta T}{\dfrac{1}{E_c}\left(\dfrac{r^2 + 1}{r^2 - 1} + \nu_c\right) + \dfrac{1}{E_t}(1 - \nu_{tt})} \qquad (2)$$

Where E_c is the modulus of elasticity of concrete ; ν_c is Poisson's ratio of concrete ; α_c is the coefficient of thermal expansion of concrete ; E_t is the modulus of elasticity of the FRP bar in the transverse direction ; ν_{tt} is Poisson's ratio of the FRP bar in the transverse direction and α_t is the transverse coefficient of thermal expansion of FRP bar.

The maximum value of the radial tensile stress in concrete at the interface, at $\rho = a$, obtained by Eq.(1), is given by:

$$\sigma_{\rho\,\max} = -P = f_{ct} \qquad (3)$$

The first circumferential cracks appear in concrete at the FRP bar/concrete interface when the radial stress reaches the tensile strength of concrete f_{ct} at the thermal load (ΔT_{cr}) obtained from Eqs. 2 and 3, as follows:

$$\Delta T_{cr} = \frac{-f_{ct}}{(\alpha_t - \alpha_c)}\left[\frac{1}{E_c}\left(\frac{r^2 + 1}{r^2 - 1} + \nu_c\right) + \frac{1}{E_t}(1 - \nu_{tt})\right] \qquad (4)$$

4 Comparison between analytical and numerical results

4.1 Cracking thermal loadings

Table 5 presents comparison between thermal loads (ΔT_{cr}) that produce the first circumferential cracks in concrete at the interface of FRP bar/concrete obtained from analytical and numerical models for prismatic concrete beams reinforced with GFRP bars that have a tensile strength of concrete $f_{ct} = 4.1$ MPa. It can be observed that the algebraic values of thermal loads ΔT_{cr} predicted from numerical model are generally lower than those determined from analytical model because of the non-linear behavior of concrete considered in the numerical model.

Table 5. Thermal load ΔT_{cr} producing the first circumferential cracks in concrete at FRP bar/concrete interface of prismatic concrete beams - comparison between analytical and numerical models
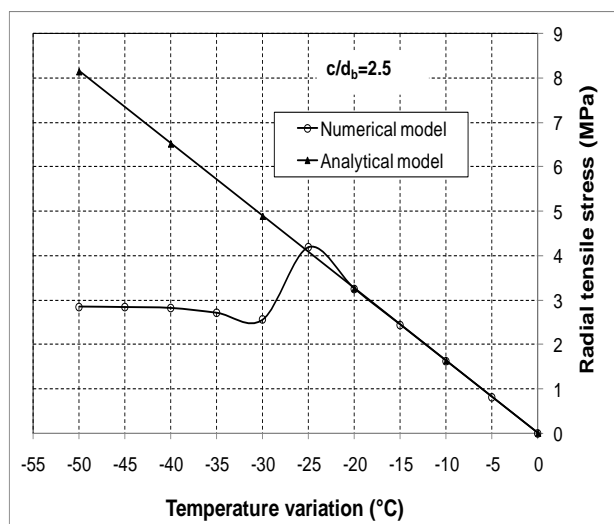
c/d_b	Analytical model	Numerical model
	ΔT_{cr}, ℃	ΔT_{cr}, ℃
$1.9 < c/d_b \leq 3.6$	-25	-25
$1 \leq c/d_b \leq 1.9$	-26	-30

4.2 Thermal stresses

Figures 6 and 7 compare typical curves of radial tensile stresses predicted from analytical model with those obtained from numerical model at FRP bar/concrete interface of prismatic concrete beams reinforced with GFRP bars that have a ratio of concrete cover thickness to FRP bar diameter (c/d_b) equal to 1.2 and 2.5. It can be seen that the numerical results predicted from the non-linear numerical model are in good agreement with analytical results until -25℃ and -30℃ from which numerical curves decrease suddenly because of the appearance of circumferential cracks in concrete which are not considered in the analytical model.
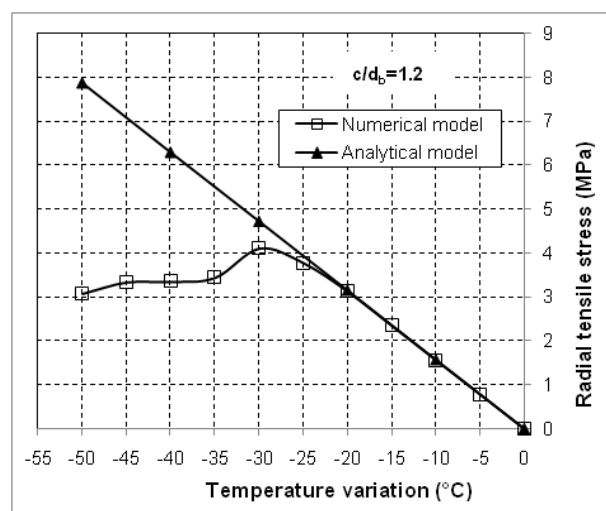
Fig. 6. Radial tensile concrete stress versus temperature variation at FRP bar/concrete interface of concrete beam having a ratio $c/d_b = 1.2$ - Comparison between numerical and analytical models

Fig.7. Radial tensile concrete stress versus temperature variation at FRP bar/concrete interface of concrete beam having a ratio c/d_b = 2.5 - Comparison between numerical and analytical models

5. Conclusions

- First circumferential cracks appear in concrete at FRP bar/concrete interface at temperature decrease ΔT_{cr} varied between -30 ℃ and -25 ℃ for prismatic concrete beams reinforced with GFRP bars having a ratio of concrete cover thickness to FRP bar diameter (c/d_b) varied from 1.0 to 3.2 and a concrete tensile strength of 4.1 MPa.

- The radial thermal stresses predicted from nonlinear numerical model, at FRP bar/concrete interface of prismatic concrete beams reinforced glass FRP bars having ratio c/d_b varied between 1.0 and 3.2, are in good agreement with those determined from the linear analytical model until a temperature variation ΔT_{cr} around -25 ℃ from which the numerical results decrease abruptly because of the appearance of circumferential cracks which are not considered in the linear analytical model.

- At low temperature, the non-linear numerical analysis shows that the depths of circumferential cracks propagated from the interface through the concrete cover increase with the decrease of the thermal load ΔT (from -25 ℃ to -50 ℃). These depths did not reach the outer surface of the concrete cover under low temperatures up to -50 ℃. Also, the radial tensile stress at FRP bar/concrete interface increases with the increase in the ratio c/d_b.

References

1. B. Benmokrane, E. El-Salakawy, and E. Ahmed, *Proceedings of the Fourth International Conference on Durability & Sustainability of Fibre Reinforced Polymer Composites for Construction and Rehabilitation,* CDCC-11, (Quebec City, Quebec, Canada, 2011).

2. A. Zaidi and R. Masmoudi, Effect of Concrete Cover Thickness and FRP-Bars Spacing on the Transverse Thermal Expansion of FRP Bars, *8th International Symposium on Fiber Reinforced Polymer Reinforcement for Concrete Structures,* (University of Patras, Department of Civil Engineering, Patras, Greece, 2007).

3. R. Masmoudi, A. Zaidi, and P. Gérard, Transverse thermal expansion of FRP bars embedded in Concrete, *Journal of Composites for Construction,* ASCE, **9** (2005), 377-387.

4. Gentry, T.R., and Husain, M., Thermal compatibility of concrete and composite reinforcements, *Journal of Composites for Construction*, **3** (1999), 82-86.

5. Canadian Standards Association, Design and Construction of Building Components with Fiber–Reinforced Polymers, *CAN/CSA–S806–02*, Toronto, Ontario, Canada, (2002).

6. Rahman, H.A., Kingsley, C.Y., and Taylor, D.A., Thermal stress in FRP reinforced concrete, *Proceedings, Annual Conference of the Canadian Society for Civil Engineering*, Ottawa, (1995), 605-614.